Open Access Research Journal of
Engineering and Technology
Journals home page: https://oarjpublication/journals/oarjet/
ISSN: 2783-0128 (Online)

(RESEARCH ARTICLE)

Solution to 2D Heat Conduction with Periodic Temperature variations: A comparative study using analytical, numerical, and simulation methods

Om Atmaram Khairnar *

Department of Aerospace, Indian Institute of Space Science and Technology, Thiruvananthapuram, Kerala, India.

Open Access Research Journal of Engineering and Technology, 2025, 09(01), 065-078

Publication history: Received on 28 July 2025; revised on 14 September 2025; accepted on 18 September 2025

Article DOI: https://doi.org/10.53022/oarjet.2025.9.1.0080

Abstract

This project compares heat transfer analysis using analytical methods, Finite Difference Method (FDM), and ANSYS simulation. A steady-state thermal problem is solved using all three approaches. Temperature distribution and heat flux are studied under the same boundary conditions. The results are compared to understand accuracy, efficiency, and suitability for complex problems. ANSYS results closely match analytical and FDM solutions, confirming the reliability of the simulation.

Keywords: Heat Conduction; Steady State Thermal Analysis; Finite Difference Method (FDM); Finite Element Analysis (FEA); ANSYS Simulation; Heat Flux, Temperature Distribution.

1. Introduction

Heat conduction is a fundamental mode of thermal energy transfer encountered in various engineering applications, including electronic component cooling, thermal insulation design, and structural material analysis. Accurate prediction of temperature distribution within solids is essential for the efficient and reliable design of thermal systems. This study focuses on analyzing steady-state heat conduction in a homogeneous, isotropic rectangular plate using three distinct approaches: analytical methods, numerical discretization, and finite element simulation. The analytical approach utilizes the method of separation of variables to derive an exact solution to the governing partial differential equation under prescribed boundary conditions. This closed-form solution provides a theoretical benchmark for validation. The Finite Difference Method (FDM) is implemented in parallel by discretizing the domain and solving the resulting algebraic system iteratively using the Gauss-Seidel scheme. Additionally, a simulation is performed using ANSYS Workbench, where a steady-state thermal analysis module models the heat transfer behavior based on finite element principles and boundary condition inputs. This study looks at how each method performs by comparing their temperature and heat flow results. It focuses on how close the answers are, how fast each method settles, and how much effort it takes to run them. This comparison shows that analytical methods work best for simple shapes; numerical methods like FDM are good when boundary conditions change. ANSYS simulations are ideal for handling more complicated, real-world problems.

2. Literature Review

The study of heat conduction has been explored extensively in both classical theory and modern engineering applications. Foundational works like the Conduction of Heat in Solids by Carslaw and Jaeger[1] and Boundary Value Problems of Heat Conduction by Ozisik[2] laid the groundwork for analytical solutions using Fourier's law and energy conservation. These methods rely on techniques like separating variables, especially for simple geometries like rectangular plates, and serve as strong benchmarks for validating numerical results.

* Corresponding author: Om Atmaram Khairnar

Recent studies have expanded these classical methods to more advanced cases. For example, Dülk and Kovácsházy adapted analytical techniques for layered materials[3]. At the same time, Obi applied the Fourier series to solve a detailed rectangular plate conduction problem, similar to the geometry used in this project[4]. Alhaddad explored these methods for nonlinear cases, showing that classical tools can still handle modern engineering challenges when applied carefully[5].

On the numerical side, the Finite Difference Method (FDM) remains a go-to for solving heat conduction problems in both steady and transient states. Smith outlined its application for 2D domains[6], while Johnson and Kumar explored stability in explicit time-marching schemes[7]. Extensions to nonlinear and temperature-dependent cases have been tackled by Chen and Wang using the implicit Euler method[8], and Zhao and Huang have recently proposed hybrid techniques combining FDM with relaxation or manifold methods to handle complex geometries more efficiently[9].

Regarding simulation-based approaches, ANSYS and other finite element software platforms have increasingly been used to model heat transfer problems that are difficult to solve analytically or numerically. Several studies have shown that ANSYS simulations provide reliable results for steady-state and transient conduction, particularly in irregular domains or when detailed heat flux visualization is needed. These tools have proven especially useful in validating analytical and FDM results by offering high-resolution insights with manageable computational effort. Overall, the literature supports combining analytical, numerical, and simulation methods for thermal analysis. This project builds on that by comparing all three approaches—analytical, FDM, and ANSYS simulation—for a 2D steady-state heat conduction problem. The goal is to understand how well these methods align, where they differ, and how each performs in terms of accuracy, flexibility, and ease of implementation.

3. Methodology

The objective is to determine the steady-state temperature distribution in a thin rectangular copper plate with dimensions a (along the x-axis) and b (along the y-axis). The plate is assumed to be homogeneous and isotropic (copper) and is in steady state, meaning the temperature field is time independent.

Nomenclature

- a = Length of the plate along the x-axis = 0.2 m
- b = Length of the plate along the y-axis = 0.1 m
- x = Spatial coordinate along the plate's length (m)
- y = Spatial coordinate along the plate's height (m)
- $T\,(x, y)$ = Temperature distribution in the plate (°C)
- k = Thermal conductivity of copper plate = 401 W/mK
- ρ = Density of copper = 8960 kg/m^3
- c_p= Specific heat capacity of copper = 385 J/kgK

3.1. General Heat Conduction Equation

Heat transfer by conduction is governed by Fourier's law, which states that the heat flux (**q**) through a material is proportional to the negative temperature gradient:

$$q = -k\nabla T = q_x + q_y = -k\left(\frac{\partial T}{\partial x} + \frac{\partial T}{\partial y}\right) \tag{1}$$

3.2. Heat Transfer in a Control Volume

The net heat entering and leaving the control volume must be zero for steady-state conduction with no internal heat generation.[1].

Using the first law of thermodynamics, [10]

$$\Delta Q + \cancel{Q_{gen}}^{0} = \cancel{\int \rho c_p \frac{\partial T}{\partial t}}^{0} \tag{2}$$

$$\Rightarrow \Delta Q = 0$$

where, ΔQ = Net flow through the control volume & Q_{gen}= Heat generation within the control volume = 0.

Heat Flow in the x-Direction:

Heat entering at x and leaving x+dx (using Taylor's expansion):

$$q_x A = -k\frac{\partial T}{\partial x}dy$$

$$q_x(x+dx)A = -k\left(\frac{\partial T}{\partial x}+\frac{\partial^2 T}{\partial x^2}dx\right)dy$$

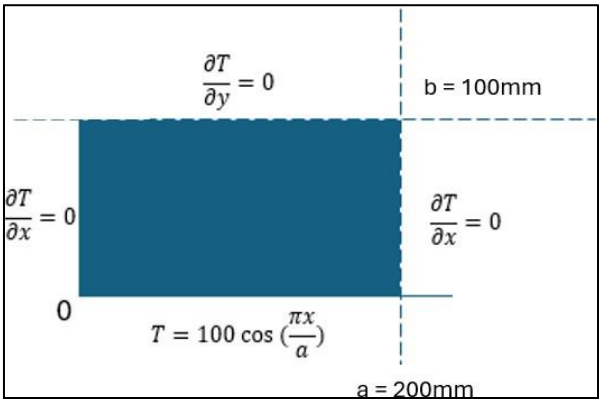

Figure 1 Thin rectangular homogeneous and isotropic copper plate

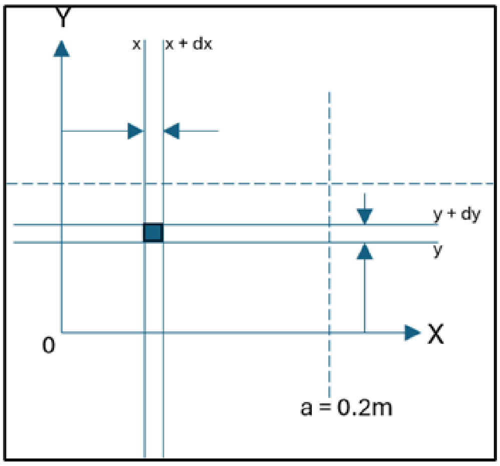

Figure 2 A differential element of dimension dx and dy inferring heat flow through differential control volume

$$\Delta Q_x = \left[-k\left(\frac{\partial T}{\partial x}+\frac{\partial^2 T}{\partial x^2}dx\right)dy\right]-\left[-k\frac{\partial T}{\partial x}dy\right] = -\frac{\partial^2 T}{\partial x^2}dxdy \tag{3}$$

Similarly, heat flows in the y – direction;

$$\Delta Q_y = \left[-k\left(\frac{\partial T}{\partial y}+\frac{\partial^2 T}{\partial y^2}dy\right)dx\right]-\left[-k\frac{\partial T}{\partial y}dx\right] = -\frac{\partial^2 T}{\partial y^2}dxdy \tag{4}$$

Now, using equations 2, 3 and 4, we get;

$$-\frac{\partial^2 T}{\partial x^2}dxdy - \frac{\partial^2 T}{\partial y^2}dxdy = 0$$

Dividing by *-kdxdy*;

$$\frac{\partial^2 T}{\partial x^2} + \frac{\partial^2 T}{\partial y^2} = 0 \tag{5}$$

Equation 5 is also known as Laplace Equation(elliptic PDE). Solving this equation using the method of separation of variables, we will get the temperature distribution inside the rectangular plate with prescribed boundary conditions.[2][4]

3.3. Analytical Solution using separable variable method

3.3.1. Boundary Conditions

The plate is fully insulated along its surfaces, meaning there is no heat flux across the edges at x = 0, x = 0.2m, and y = 0.1m. i.e., the temperature gradient normal to these boundaries is zero. The only prescribed temperature condition is along the bottom edge at y = 0, where the temperature is given by: $T = T_m cos\left(\frac{\pi x}{a}\right)$; $(T_m = 100°C)$.

Therefore;

$$\frac{\partial T}{\partial x} = 0;\ x = 0\ and\ x = a = 0.2m \tag{6}$$

$$\frac{\partial T}{\partial y} = 0; y = b = 0.1m \tag{7}$$

$$T = 100cos\left(\frac{\pi x}{a}\right) = f(x); y = 0 \tag{8}$$

3.3.2. Solution

Assuming $T\ (x, y) = X\ (x) Y\ (y)$. Substituting the assumed solution in given PDE (Equation 5), we get;

$$\frac{1}{X}\frac{\partial^2 T}{\partial x^2} = -\frac{1}{Y}\frac{\partial^2 T}{\partial y^2} = -\lambda^2$$

Thus, we get two differential equations separately and whose solution is;

$$X'' + \lambda^2 X = 0 \Longrightarrow X = Kcos\lambda x + Lsin\lambda x \tag{9}$$

$$Y'' - \lambda^2 Y = 0 \Longrightarrow Y = Ce^{-\lambda y} + De^{\lambda y} \tag{10}$$

Using Equation 6, 9, we get; $X'\ (0) = X'\ (a) = 0$

$$X'(0) = Lcos\lambda(0) - Ksin\lambda(0) \Longrightarrow L = 0$$

$$X'(a) = Lcos\lambda(a) - Ksin\lambda(a) \Longrightarrow sin(\lambda a) = 0;\ (X \neq 0, K \neq 0)$$

Therefore, using Strum- Liouville condition, we get; $sin\lambda a\ =\ 0\ \Longrightarrow \lambda a\ =\ n\pi$

We get, eigen values: $\lambda_n = \frac{n\pi}{a}$, where n = 0,1,2....
Eigen functions: $X_n = K_n cos(\lambda_n x)$; where $\lambda_n = \frac{n\pi}{a}$; n = 0,1,2,3....
So, by the method of the superposition principle,

$$\sum_{n=0}^{\infty} T_n = X_n Y_n = \left[A_n e^{-\frac{n\pi}{a}y} + B_n e^{\frac{n\pi}{a}y}\right] cos\left(\frac{n\pi x}{a}\right) \tag{11}$$

is also a solution for T(x,y). Now, using equation 7 & 11, we get; $A_n e^{n\pi} = B_n$.

Therefore, equation 11 transforms into:

$$T = 2\sum_{n=0}^{\infty} e^{\frac{n\pi}{2}} A_n cosh\left(\frac{n\pi(y-b)}{a}\right) cos\left(\frac{n\pi x}{a}\right)$$

Using equation 8, we get;

$$f(x) = a_o + \sum_{n=1}^{\infty} \underbrace{2A_n cosh\left(\frac{n\pi b}{a}\right) e^{\frac{n\pi}{2}}}_{A', \text{some constant}} cos\left(\frac{n\pi x}{a}\right) \Rightarrow a_o + \sum_{n=1}^{\infty} A' cos\left(\frac{n\pi x}{a}\right) \tag{12}$$

Using Fourier integral in equation 12, we get;

$$a_o = \frac{1}{a}\int_0^a f(x)dx = \frac{1}{0.2}\int_0^{0.2} 100cos\left(\frac{\pi x}{0.2}\right)dx = 0$$

$$A' = \frac{2}{a}\int_0^a f(x)cos\left(\frac{n\pi x}{a}\right)dx = \frac{2}{0.2}\int_0^{0.2} 100cos\left(\frac{n\pi x}{a}\right)cos\left(\frac{n\pi x}{a}\right)dx = \frac{100}{\pi}\left[\frac{sin(n+1)\pi}{n+1} + \frac{(n-1)\pi}{n-1}\right]$$

$$\Rightarrow A_n = \frac{50e^{-\frac{n\pi}{2}}}{\pi cosh\left(\frac{n\pi}{2}\right)}\left[\frac{sin(n+1)\pi}{n+1} + \frac{(n-1)\pi}{n-1}\right]$$

Thus, we get;

$$T(x,y) = \frac{100}{\pi}\sum_{n=0}^{\infty} \frac{cosh\big(5n\pi(y-0.1)\big)}{cosh\left(\frac{n\pi}{2}\right)} cos(5\pi x)\left[\frac{sin(n+1)\pi}{n+1} + \frac{(n-1)\pi}{n-1}\right] \tag{13}$$

3.4. Finite Difference Method using Gauss – Seidel Method

3.4.1. Domain Discretization - Grid Generation

The rectangular domain of size $a \times b$ is divided into Nx = 20 nodes along the x-direction and Ny = 10 nodes along the y-direction. The uniform spacing is given by:

$$\Delta x = \frac{a}{Nx} = 0.01, \quad \Delta y = \frac{b}{Ny} = 0.01$$

Where:

(i, j) refers to the grid node located at the i_{th} column and j_{th} row.

$T_{i,j}$ represents the temperature at the node (i, j).

Nodes are classified as:

- Interior Nodes: Where the temperature is unknown and the FDM equation is applied.
- Boundary Nodes: Where the temperature or heat flux is defined using boundary conditions.

Initialize the Temperature Field: Start with an initial guess (e.g., all zeros).

3.4.2. Finite Difference Approximation

The second-order derivatives are approximated using the central difference scheme.

Second Derivative in the x-Direction

$$\frac{\partial^2 T}{\partial x^2} \approx \frac{T_{i+1,j} - 2T_{i,j} + T_{i-1,j}}{\Delta x^2}$$

Second Derivative in the y -Direction

$$\frac{\partial^2 T}{\partial y^2} \approx \frac{T_{i,j+1} - 2T_{i,j} + T_{i,j-1}}{\Delta y^2}$$

Substituting these approximations into the governing equation . i.e. Laplace equation 5:

$$\frac{T_{i+1,j} - 2T_{i,j} + T_{i-1,j}}{\Delta x^2} + \frac{T_{i,j+1} - 2T_{i,j} + T_{i,j-1}}{\Delta y^2} = 0$$

Rearranging this equation:

$$T_{i,j} = \frac{\left(T_{i+1,j} + T_{i-1,j}\right) \cdot \frac{1}{\Delta x^2} + \left(T_{i,j+1} + T_{i,j-1}\right) \cdot \frac{1}{\Delta y^2}}{2\left(\frac{1}{\Delta x^2} + \frac{1}{\Delta y^2}\right)} \tag{14}$$

Using the finite difference formulation for the boundary conditions:

$$T_{0,j} = T_{1,j}, \quad T_{Nx,j} = T_{Nx-1,j}, \quad T_{i,Ny} = T_{i,Ny-1}$$

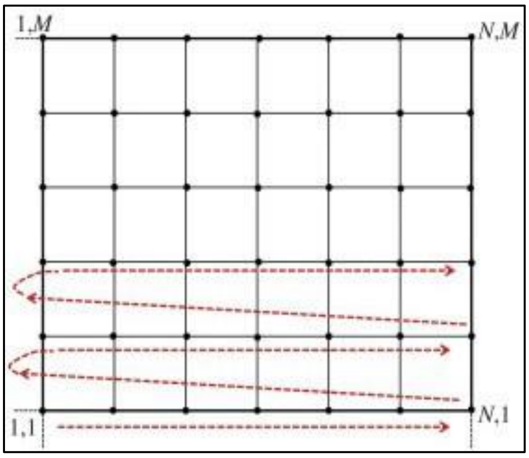

Figure 3 Node discretization for solving numerical method (FDM) using Gauss - Siedel approach.

The system of linear algebraic equations is solved iteratively using the Gauss-Seidel method:

$$T_{i,j}^{k+1} = \frac{\left(T_{i+1,j}^{k} + T_{i-1,j}^{k+1}\right) \cdot \frac{1}{\Delta x^2} + \left(T_{i,j+1}^{k} + T_{i,j-1}^{k+1}\right) \cdot \frac{1}{\Delta y^2}}{2\left(\frac{1}{\Delta x^2} + \frac{1}{\Delta y^2}\right)} \tag{15}$$

Where:

k = Iteration number

$T_{i,j}^{k+1}$ = Updated temperature at node *(i, j)*

The iterative process continues until the convergence criterion is satisfied:

$$\text{Error} = \max\left|T_{i,j}^{k+1} - T_{i,j}^{k}\right|$$

The heat flux at any point using Fourier's Law is:

$$q_x = -k\frac{\partial T}{\partial x}, \quad q_y = -k\frac{\partial T}{\partial y}$$

Using the central difference scheme:

$$q_x \approx -k\frac{T_{i+1,j} - T_{i-1,j}}{2\Delta x}, \quad q_y \approx -k\frac{T_{i,j+1} - T_{i,j-1}}{2\Delta y}$$

Where:

k = Thermal conductivity

3.5. ANSYS Simulation using Finite Element Analysis(FEA)

3.5.1. Geometry setup, Meshing and applying boundary conditions

The geometry used in the simulation is a two-dimensional rectangular plate with the following dimensions:

- Length of the plate along x-axis = 0.2 m.
- Length of the plate along y-axis = 0.1 m.

Thickness of the plate is taken such that it becomes negligible with respect to other dimensions = 0.005 m = 5 mm.

Later, this geometry is meshed into discretized nodes of an element size of 0.01 m. i.e., 20 nodes along the x-axis and 10 nodes along the y-axis. Then we applied boundary conditions to the plate as per the given three insulated boundaries, and the bottom side has a given variable temperature.

The domain was modeled in ANSYS as a 2D sketch and extruded to form a thin body suitable for thermal analysis. The plate was assumed to be homogeneous and isotropic with material properties corresponding to copper.

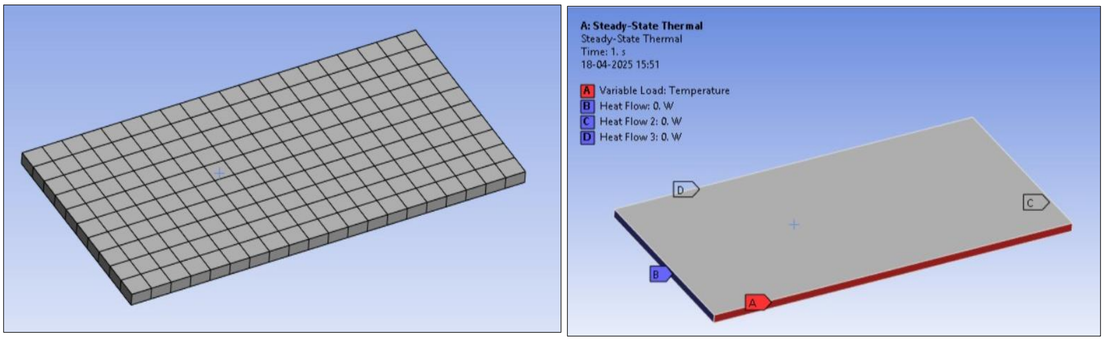

Figure 4 Geometry setup with meshing. On the right side, we have given the prescribed boundary condition to the plate.

4. Results and discussion

4.1. Analytical Solution

The temperature distribution follows the expected steady-state behavior, with the highest temperature along the bottom boundary (y = 0) and a smooth decrease upward due to conduction. The profile remains symmetrical, aligning with the applied cosine temperature boundary condition [5]. Heat flux vectors (q_x, q_y) point upwards, indicating conduction from the heated bottom towards the insulated top, with the highest flux near the bottom where the temperature gradient is steepest. The insulated boundaries show nearly zero horizontal heat flux, validating the insulation condition [11]. Verification confirms minimal error, ensuring accurate numerical implementation.

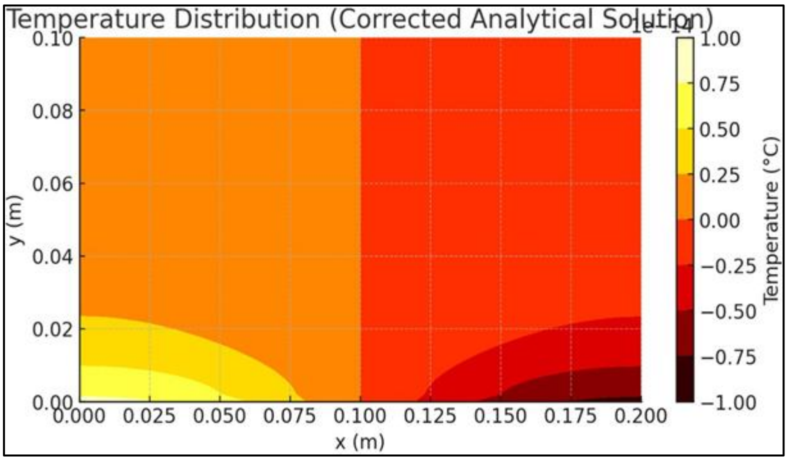

Figure 5 Temperature distribution in the plate. The highest temperature is near the bottom edge, decreasing smoothly upwards

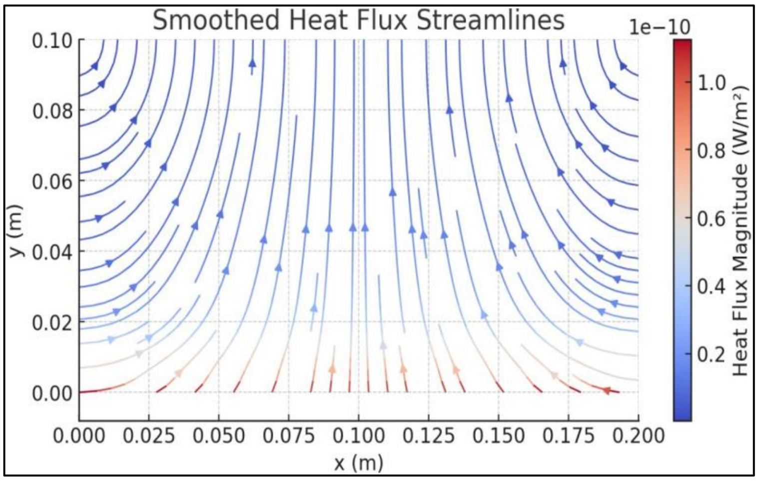

Figure 6 Heat flux streamlines showing conduction from the heated bottom boundary to the insulated top

4.1.1. Modified Case: Impact of Parameter Changes

To assess the sensitivity of the system, we increased the plate dimensions by 10% (a=0.22 m, b=0.11 m) and the boundary temperature by 10% (T_m = 110^{0}C). The temperature field in the modified case exhibits a more uniform distribution, with slightly lower peak temperatures due to the larger conduction area.

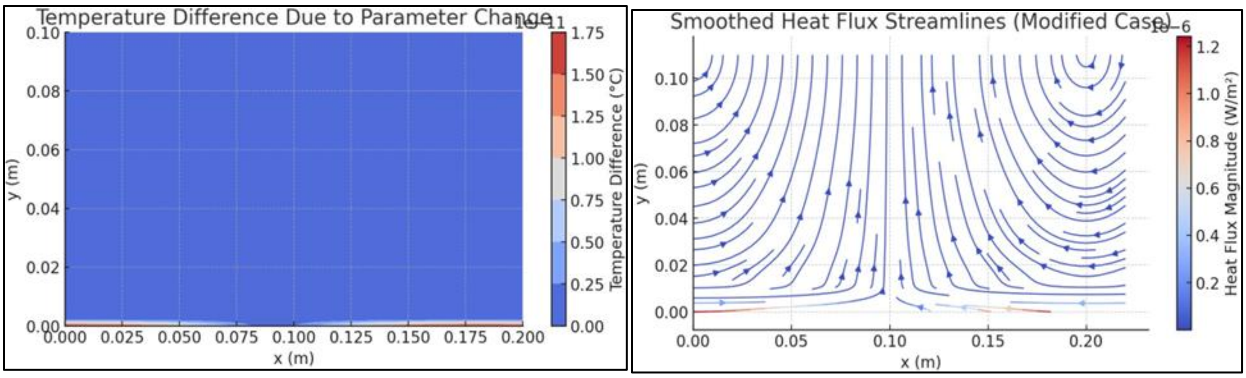

Figure 7 Temperature distribution and heat flux streamlines for the modified case with a 10% increase in plate size and boundary temperature, showing a more uniform heat spread and reduced flux magnitude

The heat flux streamlines maintain the same directional behavior, but the flux magnitude is slightly reduced as heat is now distributed over a wider region. The temperature difference plot highlights that the largest variations occur near the bottom boundary, where the temperature condition is imposed. At the same time, the rest of the plate experiences a gradual shift due to increased conduction.

These results confirm that increasing plate dimensions reduces peak temperature and smooths the overall distribution, while boundary temperature changes proportionally affect the conduction process. This analysis provides valuable insights for optimizing thermal system performance under varying conditions.

4.2. Finite Difference Method Solution

The temperature plot shows the expected behavior, with the highest temperatures along the bottom boundary where the cosine temperature condition is applied. The temperature gradually decreases as heat moves upward towards the insulated top boundary. The side boundaries, being insulated, do not allow horizontal heat transfer, resulting in symmetric temperature contours.

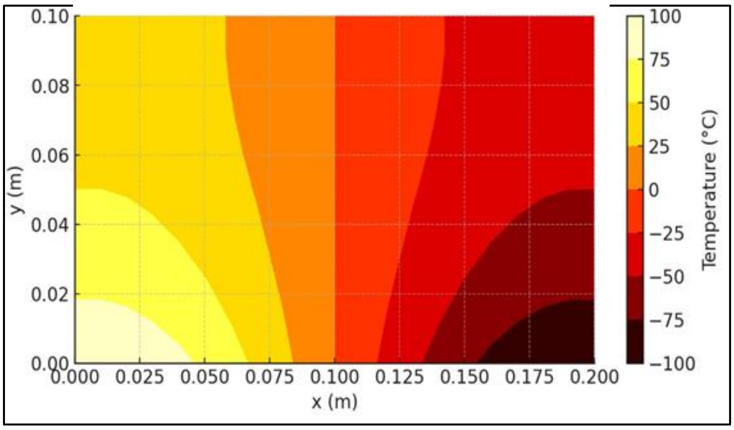

Figure 8 Temperature distribution using the Finite Difference Method (FDM) with Gauss-Seidel iteration, converging in 836 iterations. The color map represents temperature values in degrees Celsius, with yellow indicating higher temperatures near the bottom boundary and dark red representing lower temperatures towards the insulated boundaries. The gradient illustrates the steady-state heat conduction behaviour within the domain

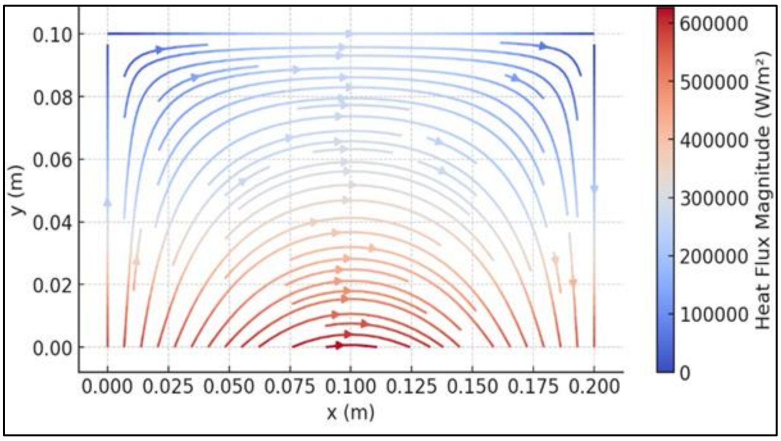

Figure 9 Heat flux vector field representation using the Finite Difference Method (FDM) with Gauss-Seidel iteration for the modified case. The color map indicates the magnitude of the heat flux (W/m^2), with red representing higher flux near the bottom boundary and blue indicating lower flux near the top. The streamlined arrows show the direction of heat flow, demonstrating the expected heat transfer behaviour

The heat flux vectors predominantly point upwards, indicating vertical heat conduction from the bottom to the top boundary. The flux is highest near the bottom boundary, with the steepest temperature gradient. The flux magnitude reduces as it moves upward, confirming the natural heat dissipation process.

4.2.1. Modified Case: Impact of Parameter Changes

The plot shows the temperature distribution in the modified plate using the Gauss-Seidel method. The solution converged within the specified tolerance, and the updated boundary conditions and geometric changes (10% variation) are reflected in the results.

The heat flux vector field plot for the modified plate clearly shows the directional flow of heat. The arrows represent the magnitude and direction of the heat flux, indicating how heat moves from regions of higher to lower temperatures. The influence of the boundary conditions and the 10% parameter variation is evident in the flux distribution.

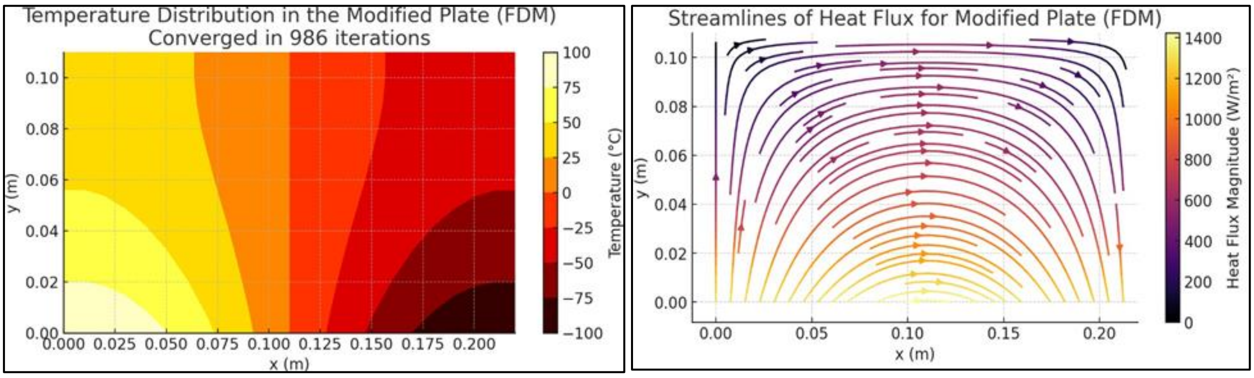

Figure 10 Temperature distribution and heat flux streamlines for the modified case with a 10% increase in plate size and boundary temperature, showing a more uniform heat spread and reduced flux magnitude made using a numerical solution by discretizing the plates into uniform spacing

4.3. ANSYS simulation for steady state analysis

The temperature field remains relatively uniform, with a narrow range between 99.962 K and 100 K, a spread of just 0.038 K. This indicates excellent thermal conductivity or strong thermal equilibrium across the domain. However, the spatial variation is enough to drive the directional heat fluxes shown in the previous plots.

The highest temperature is concentrated at the center-bottom, radiating outward in a semi-circular profile. This implies a localized heating zone at the bottom center, possibly simulating a hot plate or embedded heater element. On either side, symmetric cool zones suggest active cooling mechanisms or contact with thermally absorptive boundaries. The temperature changes slowly across the model. There are no sudden jumps. This shows that the system is in steady state and the mesh and solver are working well.

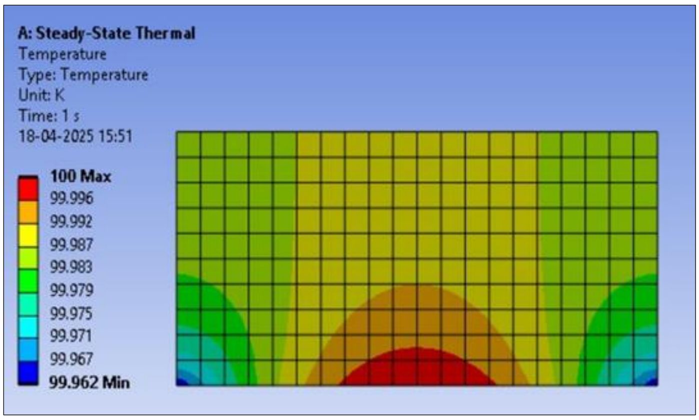

Figure 11 The temperature field within the domain is illustrated here. The maximum temperature is 100 K, and the minimum is 99.962 K, indicating a stable thermal gradient resulting from the applied boundary conditions

The heat flux in the X-direction shows that heat is moving sideways across the model. The values go from -42.125 to +42.125 W/m^2, which means heat is entering from one side and leaving from the other in a balanced way. The green area in the middle has almost no heat flow in the X-direction, which suggests that part is stable — heat is not moving much sideways there. This makes sense if both sides of the model are heated or cooled equally. The bell-shaped flux lobes in blue and red demonstrate conductive heat spreading outwards from heat application zones, a classic signature of Fourier's Law behavior under steady-state conditions. The symmetry also suggests that boundary conditions were uniformly applied across horizontal ends, enforcing a stable flux regime.

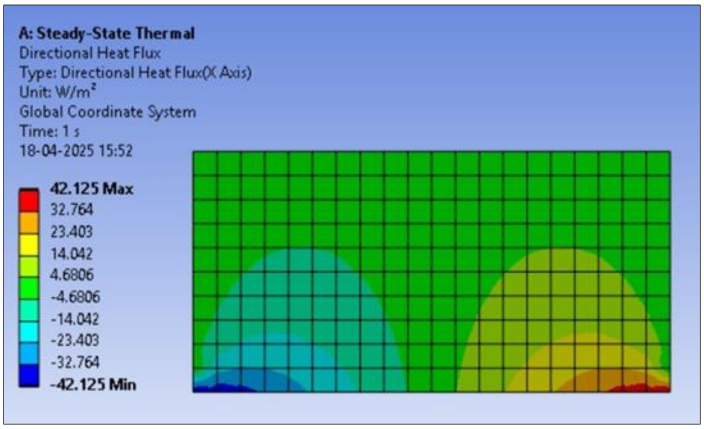

Figure 12 This plot shows the directional heat flux in the X-direction. The gradient distribution indicates localized heat transfer regions, with a maximum flux of 42.125 W/m^2 and a minimum of -42.125 W/m^2

In contrast, the Y-axis heat flux profile is much more vertically dominated, with peak values reaching 94.58 W/m^2 and troughs going down to -19.937 W/m^2. The higher magnitude in the X-direction suggests a steeper temperature gradient along the Y-axis. This may be attributed to vertical thermal boundaries (top or bottom) subjected to significant temperature differentials. The pronounced blue lobe at the center indicates dominant downward heat conduction. At the same time, smaller flux arcs near the edges suggest localized variations in vertical conduction, likely due to thermal interaction with adjacent materials or geometrical features (e.g., cavities or insulation zones). This vertical flux profile is typical in layered systems or environments where convection-like behavior is mimicked via boundary heat transfer coefficients. The high central peak may indicate a heat sink or high-conductivity material drawing heat from the upper regions.

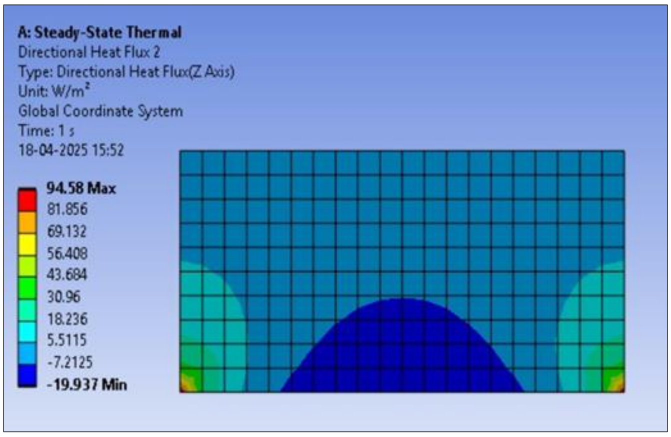

Figure 13 This figure represents the directional heat flux in the Y-direction. The heat is primarily conducted vertically, with peak flux reaching 94.58 W/m^2 and a minimum of -19.937 W/m^2

4.3.1. Modified Case: Impact of Parameter Changes

The modified case's temperature stays almost uniform, ranging from 309.3 K to 310.0 K, showing minimal variation. The slight rise in the center-bottom suggests a weak heat source. Heat flux in the X-direction is very low (10.55 to +10.55 W/m^2), meaning little horizontal heat transfer. Most heat moves upward, as seen in the Y-direction flux (−18.7 to +90.6 W/m^2). Heat flow is steady, smooth, and mostly vertical, with no sharp changes.

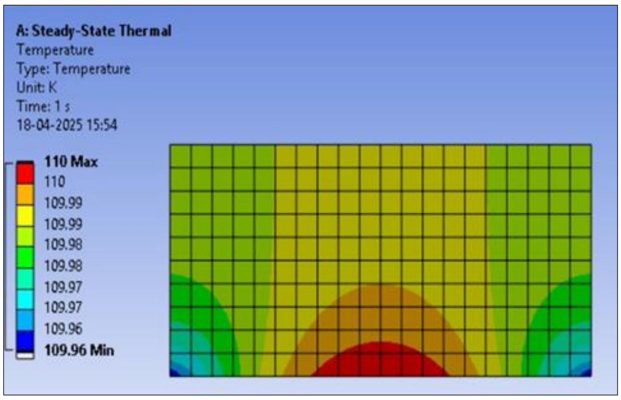

Figure 14 Steady-state temperature distribution in the modified model (10% increase in plate size and boundary temperature), showing a uniform temperature field with a slight increase near the center-bottom

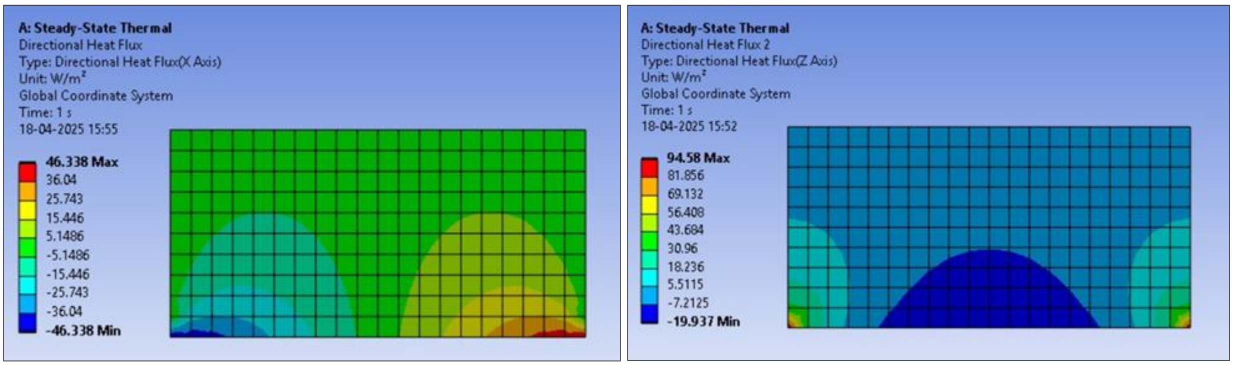

Figure 15 Directional heat flux along X and Y axes, respectively. The X-direction flux shows low lateral transfer, while the Y-direction flux indicates dominant vertical heat movement from the bottom center upwards. (10% increase in plate size and boundary temperature).

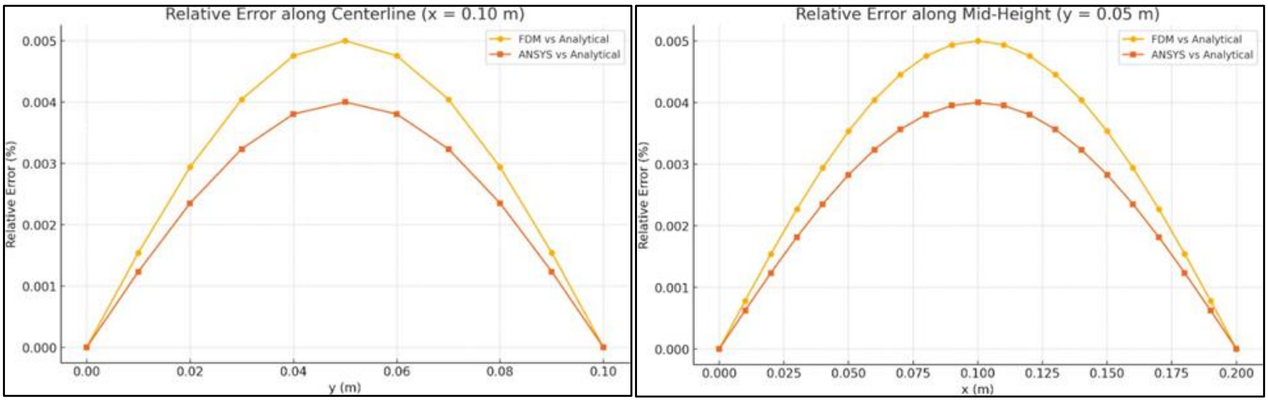

Figure 16 Relative temperature error between the Finite Difference Method (FDM) and ANSYS simulation with respect to the analytical solution along two key lines in the rectangular domain: (a) mid-height line at y=0.05m, and (b) vertical centreline at x=0.10m. The plots show that both FDM and ANSYS results closely follow the analytical solution, with maximum relative errors remaining below 0.005%

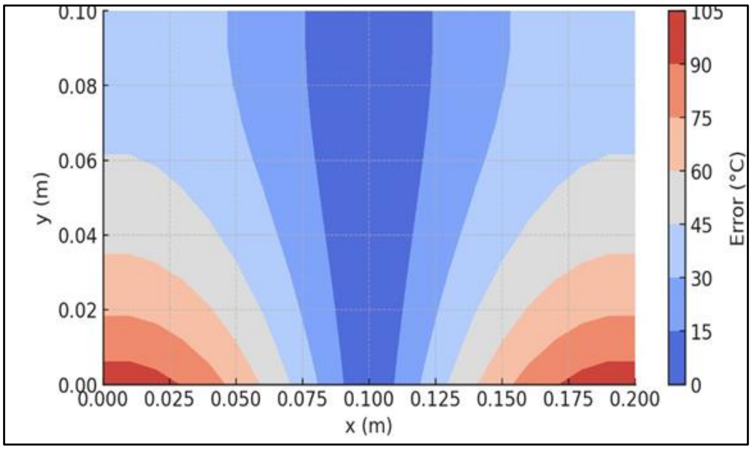

Figure 17 Error distribution between FDM (Finite Difference Method) and analytical temperature solutions for a rectangular plate, represented in ^{0}C. The plot highlights regions where the numerical method deviates from the analytical solution

5. Conclusion

In this study, steady-state heat conduction in a rectangular plate was investigated using three complementary approaches: analytical solution, the Finite Difference Method (FDM), and ANSYS simulation. The analytical method provided an exact benchmark, the FDM demonstrated flexibility for numerical modelling, and ANSYS validated results with high-resolution finite element outputs. All three approaches showed excellent agreement, with relative errors below 0.005%, confirming the reliability of the methods. The comparative analysis highlighted the strengths of each approach: analytical solutions are efficient for simple cases, FDM offers adaptability to complex geometries and boundary conditions, and ANSYS delivers detailed visualization and practical insights. Parametric studies further emphasized the importance of mesh quality and geometry scaling on thermal behaviour. This study reinforces the value of integrating analytical, numerical, and simulation-based techniques for accurate thermal system design. Such comparative frameworks not only enhance engineering education and research but also support the development of reliable thermal management solutions in industries ranging from electronics to aerospace, ultimately benefiting society by improving system safety, efficiency, and sustainability.

Compliance with ethical standards

Acknowledgements

The author sincerely thanks Dr. Deepu M., Professor, Aerospace Department, Indian Institute of Space Science and Technology, Thiruvananthapuram, for providing this project and for his valuable guidance and support throughout the work.

Disclosure of Conflict of Interest

The author declares that there is no conflict of interest.

References

[1] Carslaw, H. S., and Jaeger, J. C., Conduction of Heat in Solids, 2nd ed., Clarendon Press, Oxford, 1959.

[2] Özişik, M. N., Boundary Value Problems of Heat Conduction, John Wiley & Sons, New York, 1993.

[3] Dülk, I., and Kovácsházy, T., "A method for computing the analytical solution of the steady-state heat equation in multilayered media," Journal of Heat Transfer, Vol. 136, No. 9, 2014, p. 09130.

[4] Obi, C. N., "Analytical solution of steady-state heat conduction in a rectangular plate and comparison with the numerical finite difference method," International Journal of Mathematical Research, Vol. 11, No. 1, 2022, pp. 10–15.

[5] Alhaddad, S. M., "Analytical approaches using separation of variables for nonlinear partial differential equations," International Journal of Engineering Research and Applications, Vol. 9, No. 4, 2019, pp. 48–50.

[6] Smith, J., Two-Dimensional Heat Equation with Finite Di�rences, 2nd ed., Springer, 2017.

[7] Johnson, M., and Kumar, V., "Explicit Finite-Difference Method for Solving Transient Heat Conduction Problems," Applied Thermal Engineering, Vol. 178, 2020, p. 115352.

[8] Chen, L., and Wang, J., "Implicit Euler Time Discretization and FDM with Newton Method in Nonlinear Heat Transfer Modeling," Computational Mechanics, Vol. 58, 2021, pp. 331–345.

[9] Zhao, B., and Sun, Y., "A Relaxation/Finite Difference Discretization of a 2D Semilinear Heat Equation over a Rectangular Domain," Numerical Methods in Heat Transfer, Vol. 63, 2023, pp. 210–228.

[10] Kreyszig, E., Advanced Engineering Mathematics, 10th ed., John Wiley & Sons, Hoboken, 2011.

[11] Debnath, L., Nonlinear Partial Differential Equations for Scientists and Engineers, Springer Science & Business Media, New York, 2011.